12.3

INVITED

CONSIDERATIONS FOR INDUCTIVELY DRIVEN PLASMA IMPLOSIONS

D.L. SMITH, R.P. HENDERSON, and R.E. REINOVSKY

Air Force Weapons Laboratory
Kirtland AFB, New Mexico

Abstract

Inductive pulse forming techniques appropriate for the driving of imploding plasmas have been explored with special attention given to a suitable opening switch. Parametric investigations of circuit models indicate that imploding load performance is relatively independent of opening switch parameters. Extrapolation of existing experimental and computer simulated data leads to conceptual design criteria for a fused metal foil opening switch which will be implemented on a 1.9 MJ system. The inductive system compares favorably with the direct capacitor driven system in terms of kinetic energy with the definite advantage of shorter time scales on which the energy is delivered to the implosion.

Introduction

The Air Force Weapons Laboratory is investigating plasma implosion techniques as a desirable method for generating a very high energy density plasma suitable for use as an intense X-ray Source[1]. Under the SHIVA program experiments have been conducted in which a plasma formed from a thin freestanding, cylindrical metal or plastic film is driven to high velocities (> 20cm/µsec) by a high current from a 1.1 MJ, 1.3 µs capacitor bank. Proper choice of geometry and mass of the imploding plasma allow good (25-30%) coupling of electrical to kinetic energy and have efficient heating of the pinched plasma. Radiation outputs of 180 kJ (16% total efficiency) at powers in excess of 1.5 TW have been observed. Future experiments call for the delivery of much larger amounts of electrical energy (15-30 MJ), and implosion dynamics suggest that shorter implosion times (300ns) would be advantageous. To meet these requirements energy storage systems of conventional design would be exceedingly large and expensive. An attractive alternative technology

may be conceptually developed using inductive (magnetic) energy conditioning techniques[2,3] coupled with inertial primary energy storage[4]. The inertial primary store is essentially present technology. Therefore, the purpose of this work is to explore the potential applicability of inductive pulse forming techniques in the driving of imploding plasma loads. Special attention is paid to the development of a suitable opening switch. In this paper the inductively driven plasma implosion systems will be explored analytically and computationally through circuit models. The performance of currently available opening switches will be compared against the requirements developed in the analysis to assess the near term prospects for applying inductive techniques to large systems.

Simple Analysis

The circuit shown in Fig. 1 consists of a dc charged capacitor bank (C) discharging through a storage inductor ($L_s = L_{bank} + L_{ext}$) and a closed switch (S_1) that opens at peak current (I_o) to transfer the energy through switch S_2 to the load of initial inductance L_o. The load inductance increases subsequent to the initiation of current interruption thus corresponding to the implosion of the SHIVA load ($L(t) = L_o + \Delta L(t)$). The initially open switch (S_2) isolates the load from the system until switching time (t_s). The final load inductance is $L = L_o + \Delta L$ where

$$\Delta L = \frac{h\mu_o}{2\pi} \ln (R_o/R_f) \qquad (1)$$

The parameter h is the height of the cylindrical foil, while R_o and R_f are the initial and final cylinder radii respectively. Convergence ratios (R_o/R_f) of 12-14 are common and the shorter time scale implosion is expected to lead to a convergence

Report Documentation Page

Form Approved
OMB No. 0704-0188

1. REPORT DATE	2. REPORT TYPE	3. DATES COVERED
JUN 1979	**N/A**	**-**

4. TITLE AND SUBTITLE	5a. CONTRACT NUMBER
Considerations For Inductively Driven Plasma Implosions	5b. GRANT NUMBER
	5c. PROGRAM ELEMENT NUMBER
6. AUTHOR(S)	5d. PROJECT NUMBER
	5e. TASK NUMBER
	5f. WORK UNIT NUMBER

7. PERFORMING ORGANIZATION NAME(S) AND ADDRESS(ES)	8. PERFORMING ORGANIZATION REPORT NUMBER
Air Force Weapons Laboratory Kirtland AFB, New Mexico	

9. SPONSORING/MONITORING AGENCY NAME(S) AND ADDRESS(ES)	10. SPONSOR/MONITOR'S ACRONYM(S)
	11. SPONSOR/MONITOR'S REPORT NUMBER(S)

12. DISTRIBUTION/AVAILABILITY STATEMENT
Approved for public release, distribution unlimited

13. SUPPLEMENTARY NOTES
See also ADM002371. 2013 IEEE Pulsed Power Conference, Digest of Technical Papers 1976-2013, and Abstracts of the 2013 IEEE International Conference on Plasma Science. Held in San Francisco, CA on 16-21 June 2013. U.S. Government or Federal Purpose Rights License

14. ABSTRACT
Inductive pulse forming techniques appropriate for the driving of imploding plasmas have been explored with spe~ial a~tention given to a suitable opening switch. Parametric investigations of circuit models indicate that imploding load performance is relatively independent of opening switch parameters. Extrapolation o~ existing experimental and computer simulated data leads to conceptual design criteria for a fused metal foil opening switch which will be implemented on a 1.9 MJ system. The inductive system compares favorably with the direct capacitor driven system in terms of kinetic energy with the definite advantage of shorter time scales on which the energy is delivered to the implosion.

15. SUBJECT TERMS

16. SECURITY CLASSIFICATION OF:			17. LIMITATION OF ABSTRACT	18. NUMBER OF PAGES	19a. NAME OF RESPONSIBLE PERSON
a. REPORT **unclassified**	b. ABSTRACT **unclassified**	c. THIS PAGE **unclassified**	**SAR**	**8**	

Standard Form 298 (Rev. 8-98)
Prescribed by ANSI Std Z39-18

of 20. Several assumptions are employed in the simplest analysis. The final resistance of the opening switch is assumed to be large compared to the final $\dot{L}$ of the load to prevent significant sharing of current through the switch. If the imploding cylinder radius and velocity are $r(t)$ and $v(t)$, one can write

$$\dot{L}(t) = \frac{\mu_o h}{2\pi} \frac{v(t)}{r(t)} , \qquad (2)$$

It is also assumed that the resistance rises quickly, in other words that the switching time is much less than the implosion time.

At peak current and for the short energy transfer times of interest the bank voltage and the amount by which the charge on C can change is near zero, hence for the analysis the capacitor element can be represented by a short circuit. Assuming conservation of magnetic flux, the energy stored in L_s and L_o immediately after t_s is

$$E_1 = \frac{L_s}{L_s + L_o} E_o \qquad (3)$$

where E_o $(= \frac{1}{2} L_s I_o^2)$ is the energy stored in L_s prior to t_s. The energy dissipated in the rising switch resistance must be

$$E_{sw} = \frac{L_o}{L_s + L_o} E_o \qquad (4)$$

according to conservation of energy. To minimize the switch dissipation L_o must be as low as possible $(L_o << L_s)$. After the implosion the approximate energy stored in L_s, L_o, and ΔL is

$$E_2 = \frac{L_s}{L_s + L_o + \Delta L} E_o . \qquad (5)$$

The kinetic energy coupled to the plasma shell during the implosion is just the difference $E_1 - E_2$, and a kinetic efficiency can be defined as

$$\eta_{ke} = \frac{E_{ke}}{E_o} \approx \frac{\Delta L}{L_s + \Delta L} , \qquad (6)$$

if $L_o << L_s$. If $\Delta L >> L_s$ efficiency approaching unity can be realized. Thus, in general, to get most of the stored energy into kinetic energy and maximize efficiency requires $L_o << L_s << \Delta L$. Unfortunately L_o is typically fixed by consideration of power flow in the load and ΔL is fixed by the convergence

ratio and the foil height. For the SHIVA system values of L_o below 3-5 nH are unrealistic, while ΔL can range from 6 to 24 nH, and reaching very high efficiency will be difficult. Given practical constraints upon L_o and ΔL, the value of L_s remains as one parameter which can be adjusted. Intuitively, if L_s is chosen to be very small, a large amount of energy is lost in the switching operation, if it is chosen to be large the energy transfer to the load suffers. To find the optimum choice of L_s one can take $d\eta_{ke}/dL_s$ and set the result equal to zero. This results in a criterion on L_s, namely:

$$L_s = \sqrt{L_o^2 + L_o \Delta L} . \qquad (7)$$

Clearly for the case of the static load, $\Delta L = 0$, Eq. (7) gives $L_s = L_o$. Thus, the familiar static result is recovered, and as expected, from Eq. (3) and Eq. (4) $E_1 = E_{sw} = 50\% E_o$. Plotting η_{ke} as a function of L_s for an implosion where $\Delta L = 12$ nH shows that the efficiency of coupling inductive to kinetic energy goes through a maximum at the predicted optimum L_s and that the optimum is broad and relatively insensitive to small variations in L_s.

For one class of opening switches, namely electrically exploded conductors, the operation of the switch is determined by the energy, (and to some extent power history) dissipated in the switch. Therefore it is useful to characterize the circuit performance in terms of the energy dissipated in the switch given by Eq. (4). Figure 2 is a plot of the minimum dissipation fraction defined as

$$\delta = \frac{E_{sw}}{E_o} = \frac{L_o}{L_s + L_o} . \qquad (8)$$

When L_s is chosen by Eq. (7), Eq. (8) indicates that δ is only a weak function of ΔL. For small ΔL the curve approaches 50% as expected for a static load. The significance of δ is that it represents the minimum amount of energy that will be dissipated when the switch opens (at least 25% for practical cases), regardless of the characteristics or relative time of the operations of switches S_1 and S_2. Conversely it is the minimum energy available to use to actuate a dissipation driven switch. The temptation is to develop a switch which "requires"

very littly energy. Figure 2 indicates that, for example, for typical SHIVA parameters L_o = 5 nH and ΔL = 12 nH, almost 40% of the energy goes into the switch regardless of how clever the design. On the other hand, since dissipatively operated current interrupting switches may require more than the minimum energy given by δ, the fraction f of the inductively stored energy remaining after switching that is coupled to kinetic energy is also a relevant parameter. Using Eq. (3) and (5)

$$f = \frac{E_{ke}}{E_1} = 1 - \frac{L_s + L_o}{L_s + L_o + \Delta L} . \quad (9)$$

Figure 3 is a plot of the coupling fraction f. The plot shows that for realistic values of 3 nH$< L_o <$ 5 nH and for ΔL = 12 nH approximately half of the energy remaining after switching is coupled to kinetic energy yielding for these parameters an overall η_{ke} of 30%. From this simple analysis, a few design criteria emerge:

 i) Minimize L_o, as much as possible,
 ii) Maximize ΔL,
 iii) Choose $L_s \approx \sqrt{L_o^2 + L_o \Delta L}$,
 iv) Determine the dissipated switch energy.

Numerical Results

In this section, the numerical solution to a circuit similar to that in Fig. 1 is discussed. Values were chosen for circuit elements which correspond to parameters of the SHIVA-I' capacitor bank system. The 267 μF capacitor is charged to 120 kV storing 1.9 MJ. The load is modeled as a time varying resistance, having the same form as Eq. (2), in series with a time varying inductance expressed by

$$L(t) = \frac{\mu_o h}{2\pi} \ln (R/r(t)). \quad (10)$$

The radii of the return conductor (chamber) and of the imploding foil are represented by R and r(t), respectively. The initial foil radius was chosen at 5 cm and the height at 2 cm by stability arguments. The return conductor radius was chosen at 17.5 cm to give an initial value for the L of 5 nH, which corresponds to L_o = 5 nH in the analytic model. The assumption of 20:1 conversion leads to a minimum radius of 2.5 mm; a final value L_f of 17 nH; and a ΔL of 12 nH. Thus from L_o and ΔL a value of the

storage inductance is chosen from Eq. (7) to be 9.2 nH. The series output switch is modeled as a time varying resistor whose value is 1 megohm prior to switching time t_s and changes to 0.1 milliohm in 5 ns subsequent to t_s. The current interrupting switch is a resistance (R_1) which is varied as a problem variable. The opening switch inductance is typically taken as less than 1 nH but will depend on the switch geometry. The fuse inductance was included in the bank side of the circuit rather than in the fuse branch because, with the coaxial SHIVA arrangement, L_F stores magnetic energy that is available to the load when switching occurs. The circuit was subjected to numerical analysis using a circuit solving code for a variety of R_1 profiles and time scales and for a variety of switch times t_s.

Terminal Resistance

Assuming all the stored energy is transferred to the inductors, the coupled kinetic energy should be 570 kJ (30% kinetic efficiency). Choosing 33 cm/μs final velocity and allowing a 2.5 mm final radius the foil mass and final L should be 10^{-5} kg and 0.5 Ω. The constant flux analysis implied that the final value of R_1 should be much greater than 0.5 Ω to assure that most of the current is flowing in the load. To model the situation a linear ramp resistance profile was chosen (since other shapes effected only a few percent variation in the kinetic energy), changing R_1 from the initial resistance ($R_i \approx 0$) at t_1 = 2.46 μs (time of peak current) to a final terminal resistance (R_f). The switch duration (Δt) was taken as 100 ns to assure that $\Delta t <<$ t_{imp}, and R_f was varied from 30 mΩ to 5 Ω. The time at which the output switch closed (t_s), was a constant at 2.465 μs. Figure 4 shows a plot of the kinetic energy coupled to the imploding foil and the final velocity of the foil when it had collapsed to

a radius of 2.5 mm as a function of R_f, the final switch resistance. As anticipated the kinetic energy coupled at lower values of R_f is lower than that observed at higher values. Perhaps surprising is the fact that when $R_f \sim \dot{L}$ peak nearly 90% of the kinetic energy predicted by the flux model is observed coupled in the numerical solution. But when R_f drops more than an order of magnitude to 30 mΩ the kinetic efficiency decreases only moderately to 62% of the efficiency predicted by the flux model. This relatively moderate impact of reducing R_f can be motivated by referring to Fig. 5 where the dissipative impedance (RLD) and $R_1(t)$ are plotted as functions of time for the case where R_f = 30 mΩ. The plot shows that the dissipative part of the load impedance RLD rises rapidly at the very end of the implosion, and even for very modest values of R_f, RLD is less than R_f for about 90% of the implosion time. Although it is also true that most of the kinetic energy is coupled late in the implosion, it must be noted that once R_1 interrupts the current and "charges" the load inductance, the time scale (L/R_1) for current to transfer back to R_1 is much longer than the 30-60 ns for which the load impedance is higher than R_f. Coupling to L is independent of R_f until late in the implosion, and most of the necessary energy has been loaded into L (which has increased to almost $L_o + \Delta L$ before $\dot{L}$ overtakes R_f). Figure 4 also exhibits a fall off of η_{ke} above approximately 0.5 Ω. This result is perhaps more surprising than the relative moderate fall off at low R_f. At larger values of R_f excessive energy is dissipated in the fuse during opening time thus leaving less energy in the magnetic circuit to drive the implosion and thereby explaining lower overall efficiency. The conclusion is that, for implosion parameters discussed and for values of R_f that are greater than the initial $\dot{L}$ of the load (a few milliohms) but not much greater than the final $\dot{L}$ (one-half ohm), performance seems to be predicted by the simple model within about 20%. Thus the criteria results with $\dot{L}_o \ll R_f \sim \dot{L}_{pinch}$.

Output Switch Closure Time

It was observed that earlier "closing times" (t_s)

of the series output switch R_2 resulted in improved efficiency and decreased dissipation of large values of R_f. In fact the kinetic energy approaches the 570 kJ flux model value. Presumably when $\dot{R}$ is very large (i.e., R_f is large and Δt is fixed), the time scale of current transfer is seriously effected by the R_2 closing time and thus results in larger dissipation in R_1. Closing the output switch late in the interruption may be expected to result in excessive energy dissipation in the fuse and hence lower kinetic efficiency. On the other hand, closure of the output switch too early may be expected to result in lower voltages across the load and hence lower initial $\dot{I}$, and perhaps result in longer implosion time for a given load. Fortunately, from a practical point of view, the earliest possible closure time (after start of interruption time) appears most promising according to both the efficiency and implosion time. The 5 ns value of R_2 used to generate the data in Fig. 4 is more representative of practical multi-channel switches than is the less than 1 ns value required to achieve flux model efficiency. The implication is that a "low jitter" output switch is required if large values of R_f are achieved by the fuse. Figure 6 shows a plot of kinetic energy and implosion time as functions of output switch time for a case where R_f equals 500 mΩ. The implosion mass was 1×10^{-5} kg, and the switch opening time (Δt) was 100 ns. For reference, the fuse resistance profile is also sketched. The figure shows that both kinetic energy and implosion time are sensitive to switch closure time. As expected kinetic energy drops and implosion time increases with later closing times. The implosion time shows a tendency to flatten out for closure times near the start of the interruption (2.46 us).

Opening Time

The simple flux model presumes that the implosion is carried out in two steps. First a current interruption occurs, then an implosion phase occurs. The energy transfer is calculated on the assumption that $L(t)$ does not change during the interruption phase (i.e., a static load). The numerical analysis shows that for time scales of about 3/4 of the implosion time the opening switch is seeing a constant $L(t)$

(to within 25%) before it starts increasing rapidly. It also shows virtually no change of kinetic energy for time scales up to 300 ns which is very close to 75% of the implosion time. For opening times up to 500 ns the loss of efficiency is less than 5% and the implosion time lengthens somewhat (from 450 to 550 ns).

Implosion Mass/Final Velocity

One of the advantages of inductively driven implosion systems is the fact that at least in the simplest model the kinetic energy coupled is dictated only by the inductance ratios and is independent of the implosion mass. This allows relatively wide variations in final velocity to be achieved independent of kinetic energy and hence allows assessment of the effect final velocity has on the thermalization process. Figure 7 is a plot of the kinetic efficiency, final velocity, and implosion time as a function of implosion mass. The plot shows that for a full order of magnitude change of implosion mass (5×10^{-5} to 5×10^{-6} kg) the change in velocity is given by the anticipated $\sqrt{10}$ factor ranging from 11.9 cm/μs to 37.3 cm/μs. As expected the implosion time varies over a similarly wide range associated with the changing final velocity. For larger masses and for small masses, the kinetic efficiency suffers somewhat. Consideration of the circuit model shows that for the large masses the long implosion time leads to reverse charging of the bank capacitance (because a relatively large current is flowing in the "positive" direction for a long time after current peak). The energy stored in the recharging capacitor is approximately 3 times the observed loss in kinetic energy. For small values of mass the more dramatic loss results from excessive energy dissipation in the fuse resistance caused by larger values of RLD at earlier times in the implosion.

Conceptual Design

Finally, it is appropriate to consider the prospects for the success of a high energy inductive store/opening switch system as a driver for a practical imploding plasma load. Significant data has been published on the behavior of exploded foil fuses used as opening switches, but in general the

energy level (25 kJ) and the time scale (10 to a few hundred μs) are not representative of the behavior of the fusing element in systems of interest (2 MJ, 1-2 μs). The work most nearly approaching these parameters is that performed by the AFWL at the 200 kJ, 3-4 μs level. Preliminary work on a 100 kJ, 100 kV, 1.2 μs system has produced 150 to 200 ns fuse voltage risetimes achieving final fuse resistance values greater than 160 mΩ[5]. The corresponding resistivity of about 400 mΩ-cm agrees satisfactorily with previous empirical data and the models used in this paper. In this section the results of these efforts will be examined in light of the foregoing analyses and circuit calculations. Figures 8 and 9 are extracted from previous AFWL work and show current and voltage profiles for a set of copper foil fuses quenched in glass beads for a variety of physical lengths and widths which maintain a constant total fuse mass of 25 g (for 1 mil or .0254 mm thickness). For both figures the peaks occurring later in time correspond to decreasing lengths and increasing widths. Based on preceeding analyses the most promising choice for a fuse might be the fuse which produces the highest storage current while still opening in times less than (but not necessarily much less than) the implosion time. It is convenient to accept the FWHM of the voltage pulse as one measure of opening time when resistance data is not readily available. From Fig. 9 it is apparent, as expected, that the shortest interrupt time is associated with the highest peak voltage (maximum $\dot{I}$) but not with the maximum storage current. Thus compromise will be in order. For the purpose of this analysis it was chosen to discuss the maximum voltage case. The FWHM of this case is 370 ns which is acceptable for driving a 400-450 ns implosion.

For scaling purposes we resort to Maisonnier's analysis[2] which suggests a cross-sectional area for a fuse based on the parameters of the driving current and on the physical properties of the fuse of interest.

$$s^2 = \frac{W^{3/2}}{V \, L^{\frac{1}{2}} k_1 a} \tag{11}$$

where s = cross section of fuse (m^2), W = stored

energy (J), L = total system inductance (H), V = charge voltage of capacitor bank (V), and k_1a = set of parameters describing the material (= 1.2×10^{17} for copper). For the data in Figs. 8 and 9, W = 200 kJ, V – 50 kV, and L = 67 nH. Thus Eq. (11') would predict s = $7.6 \times 10^{-6} m^2$. The fuse in question was 21 cm wide and 1 mil thick so that s = .053 cm^2 or roughly 70% of that predicted by the Maisonnier model. Scaling upward for a system where W = 2 MJ, V = 120 kV, and L = 9.2 nH. 70% of the predicted area s is = .32 cm^2. A copper foil 1 mil thick would then be only 1.3 m wide. Figure 10 shows a plot of material resistivity ρ vs specific energy dissipated in the fuse. The functional relationship between ρ and specific energy is open to question but for simple approximations the empirical data of Fig. 10 will be used. Recalling that the previous analysis indicated that 670 kJ must be dissipated in the fuse, and taking approximately 6 kJ/g as the upper limit of useful specific energy from Fig. 10 indicates that 112 grams of material could be utilized. At a density of 8.94 g/cc and a cross section of .32 cm^2, this implies a fuse length of 39.2 cm. If it reaches a maximum resistivity of 520 $\mu\Omega$-cm, the fuse that is .32 cm^2 x 39 cm has a peak resistance of 63 mΩ. From Fig. 4 a fuse with R_f of 63 mΩ would drive an implosion to better than 400 kJ of kinetic energy or 20% overall kinetic efficiency. One must note that the interpretation attached to the data in Fig. 10 is conservative because the resistivity curve appears to be clearly steepening (not yet having reached the plateau assumed in our model of R_f). On the other hand Fig. 4 shows that while increasing resistivity (or increasing R_f) will help somewhat the marginal gains are small.

In conclusion, it appears that simple extrapolation of already existing data leads to a conceptual design for a fused opening switch which can be implemented on a 2 MJ system. The resulting plasma implosion should be compared against that which can be obtained by directly driving the plasma from the capacitive energy storage. Using a initial SHIVA load foil geometry of 7 cm radius and 2 cm height, and requiring for stability reasons that

the direct driven implosion be complete in less than 1.4 μs, results in the coupling of approximately 400 kJ of kinetic energy to the implosion. This performance compares very favorably with the 400+ kJ of kinetic energy implied in the previous inductive storage analysis. The advantage of the inductive system is clearly the time scale on which the energy is delivered. The inductive system promises 400 ns implosions or a factor of 3 or more faster than the direct driven implosions. At this point it appears that significant gains in thermalization and radiation are to be achieved by this modest reduction in implosion time.

References

1. W.L. Baker, M.C. Clark, J.H. Degnan, G.F. Kiuttu C.R. McClenahan, and R.E. Reinovsky, "Electromagnetic-Implosion Generation of Pulsed High-Energy-Density Plasma," J. Appl. Phys., 49, pp. 4694-4706, September 1978.

2. Ch. Maisonnier, J.G. Linhart, and C. Gourlan, "Rapid Transfer of Magnetic Energy by Means of Exploding Foils", Rev. Sci. Instrum., 37, pp. 1380-1384, October 1966.

3. J.N. DiMarco and L.C. Burkhardt, "Characteristics of a Magnetic Energy Storage System Using Exploding Foils", J. Appl. Phys., 41, pp. 3894-3899, August 1970.

4. K.I. Thomassen, "Conceptual Engineering Design for a One-GJ Fast Discharging Homopolar Machine for the Reference Theta-Pinch Fusion Reactor Semi-Annual Report EPRI ER-246, August 1976.

5. R.P. Henderson, D.L. Smith, and R.E. Reinovsky, "Preliminary Inductive Energy Transfer Experiments", Paper 15.1 in these proceedings.

6. C.R. McClenahan, J.H. Goforth, J.H. Degnan, B.M. Henderson, W.R. Janssen, and W.E. Walton, "200 Kilojoule Copper Foil Fuses", Report AFWL-TR-78-130, Air Force Weapons Laboratory, Kirtland AFB, NM, April 1978.
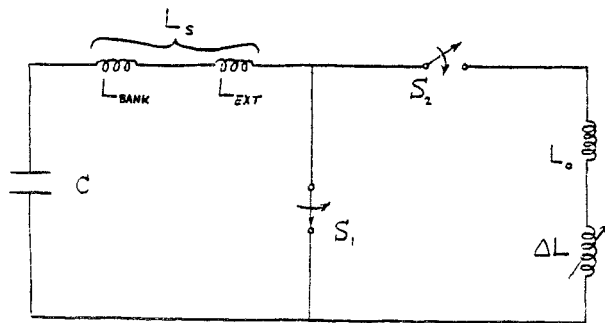
Fig. 1. Practical Circuit Representation.
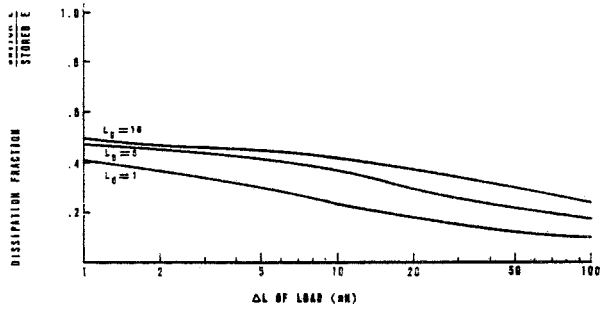
Fig. 2. Dissipation versus the Change in the Load
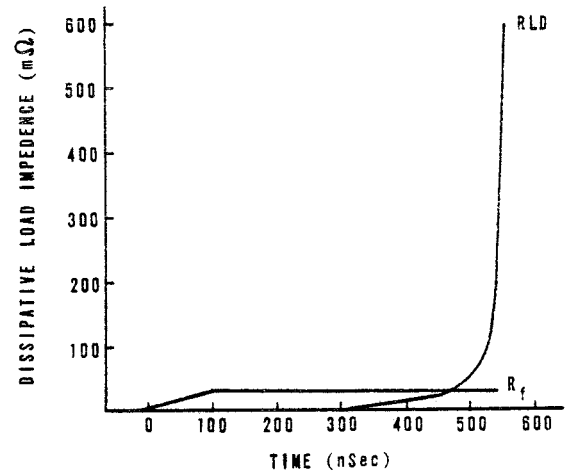   Inductance.

Fig. 5. Dissipative Load Impedance versus Time.
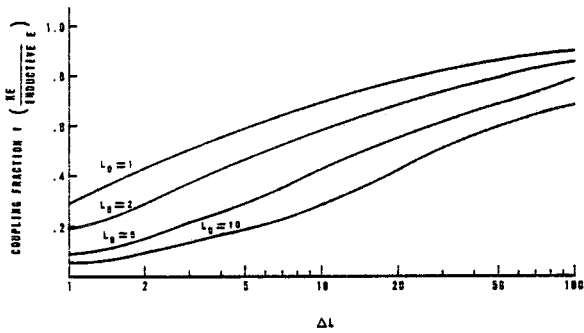

Fig. 3. Coupling Fraction versus the Change in
         Load Inductance.
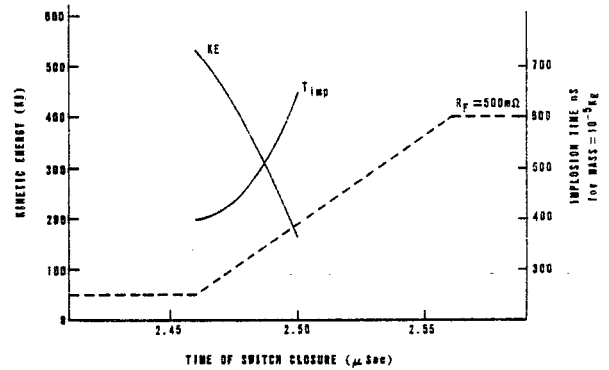

Fig. 6. Kinetic Energy and Implosion Time versus
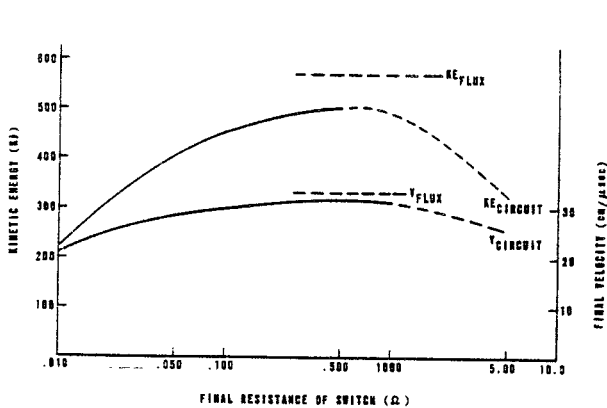   Output Switch Time.

Fig. 4. Kinetic Energy and Final Velocity of the
         Imploding Foil versus the Final Switch
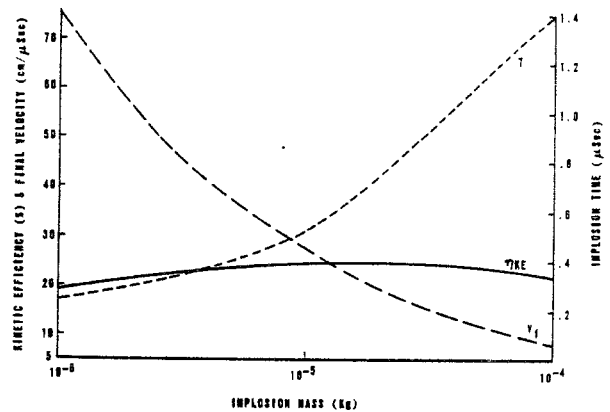   Resistance.

Fig. 7. Kinetic Efficiency, Final Velocity, and
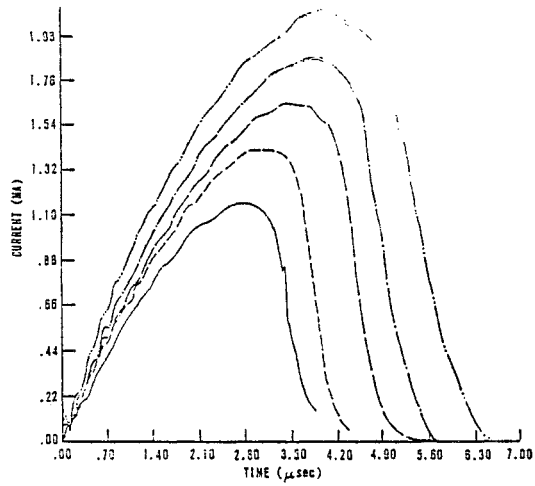   Implosion Time as a Function of Mass.

Fig. 8. Current Data for 25g Copper Foil Fuses.
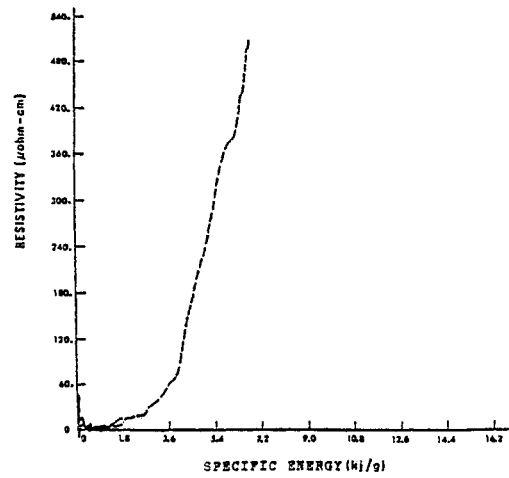

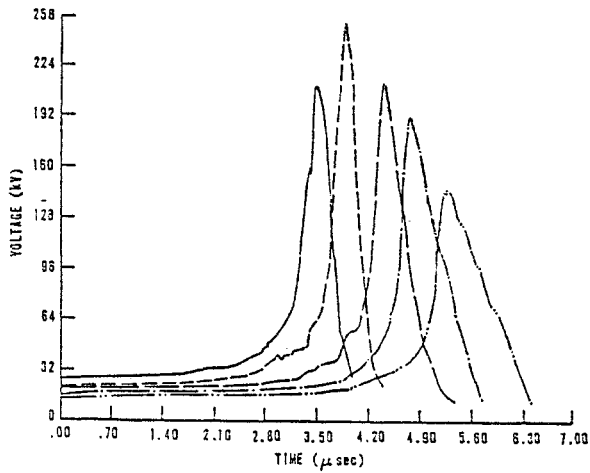Fig. 10. Resistivity versus Specific Energy in a
25.9g Copper Fuse.

Fig. 9. Voltage Data for 25g Copper Foil Fuses.